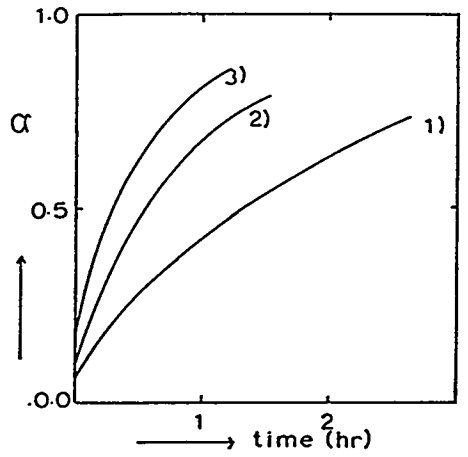

Figure III.39. Growth curves in seeded solutions at 85°C. For details see text. 1. α_o = 0.06, pH 0.86. 2. α_o = 0.09, pH 0.97. 3. α_o = 0.16, pH 1.10 (from reference III.12).

As already mentioned the seed experiments were performed under conditions such that the total surface remained approximately constant. The growth analysis is thereby simplified in comparison with a similar analysis in seed-free solution which resulted in Eq. [III.12]. Assuming that all other conditions during growth are identical in both cases, then the appropriate equation for growth of hematite in seeded solutions at constant pH shows that

$$\log(d\alpha/dt) = \log k_m + m \log(1-\alpha) \qquad \text{[III.44]}$$

In this expression k'_m will also depend on the total surface, and therefore on the amount of seed particles added to the supersaturated solution.

On replotting the experiment growth curves (Figure III.39) according to Eq. [III.44] (-log ($d\alpha$/dt) versus -log (1-α)) reasonable straight lines are obtained (see Figure III.40) which enable the evaluation of m and k'_m. The latter parameters are

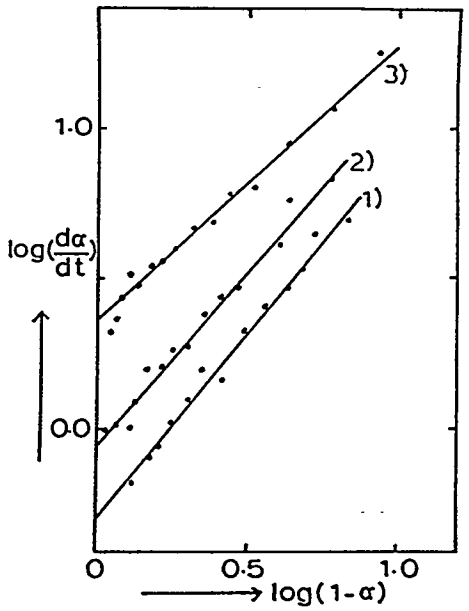

Figure III.40. Analysis of relaxation in seed experiments at 85°C according to Eq. [III.44] (from reference III.12).

listed in Table III.7. The results of a few measurements under identical conditions at 95°C are also included in Table III.7. On excluding the experiment at $\alpha_o = 0.20$ an

Table III.7

Analysis of Seed Experiments at 85 and 95°C with Aid of Eq. [III.44]

85°C				95°C			
pH	α_o	m	log k'$_m$	pH	α_o	m	log k'$_m$
0.86	0.06	0.91	-0.36	0.86	0.07	1.1	0.1
0.90	0.07	0.93	-0.09	0.98	0.13	1.35	0.47
0.97	0.09	1.1	0.05	1.03	0.20	1.3	0.75
0.99	0.10	1.06	0.19				
1.05	0.13	1.1	0.2				
1.10	0.16	1.25	0.3				
1.16	0.20	1.9	0.5				

"order" m = 1.1 $\pm$ 0.2 is obtained at 85°C. A plot of log k'_m versus pH allows one to determine the growth reaction order with respect to the hydroxyl ion. From the data at 85°C (Table III.7) this order is found to be 2.6 $\pm$ 0.5. From the data at 95°C "orders" m = 1.2 $\pm$ 0.2 and N_{OH} = 3.1 $\pm$ 1 can be obtained.

III.H. Thermal Transformations and Decompositions

Geothite (α-FeOOH) is the most stable of the various FeOOH compounds. Studies have been reported for the transformation of γ- and δ-FeOOH to geothite, and representative data are summarized below.

III.H.1. Transformation of β-FeOOH

β-FeOOH appears to transform to α-Fe_2O_3 upon heating (III.30; III.47-III.49) but little appears to have been done to define the physical properties associated with the change.

III.H.2. Transformation of γ-FeOOH

Naono and Nakai followed (III.59) the thermal decomposition of γ-FeOOH. TG curves of sample D (Figure III.41) were measured *in vacuo* by using a vacuum balance. After each powder sample had been degassed at room temperature *in*

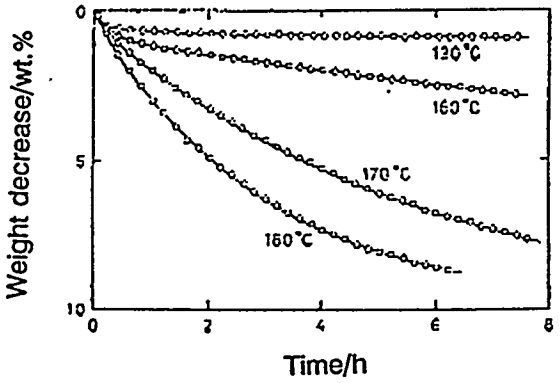

Figure III.41. TG curves of sample D at temperatures from 130 to 180°C. Surface area of sample D is 25 m^2/g (from reference III.59).

vacuo, it was isothermally decomposed between 130 and 180°C. Decomposition of γ-FeOOH scarcely occurs at 130°C, though the slight decrease of weight due to the loss of tightly adsorbed water is detected at an initial 10 min. The decomposition reaction becomes appreciable at temperatures higher than 160°C and the rate of decomposition increases with temperature. That the decomposition temperature depends remarkably on the particle size has been pointed out by Giovanoli and Brütsch (III.63; III.64), i.e., the sample having 119.4 m^2/g decomposes at 77°C, while the sample with 18.4 m^2/g decomposes at 150°C. Taking the surface area into account, the data in Figure III.41 are in approximate agreement with those of Giovanoli and Brütsch.

Figure III.42 shows power X-ray diffraction patterns of γ-FeOOH (sample D) and its decomposed products (samples E-H). For the 180°C-treated sample (sample

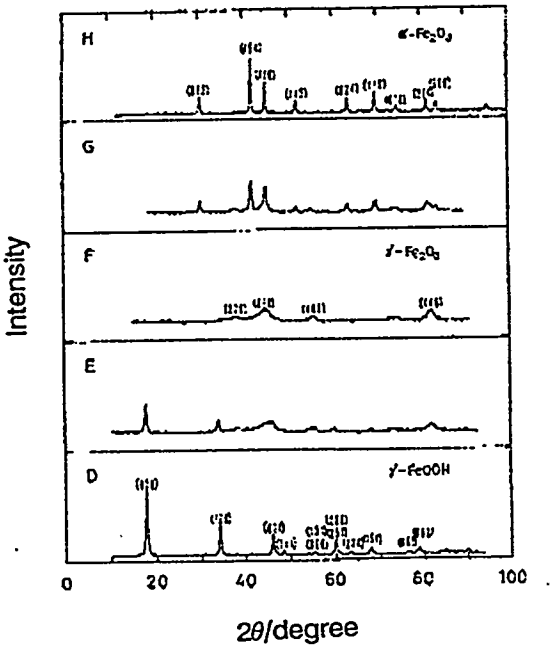

Figure III.42. Powder X-ray diffraction patterns of undecomposed γ-FeOOH and its decomposed products pretreated *in vacuo* at various temperatures. (D) undecomposed sample, (E) 180°C, 4 hr., (F) 200°C, 3 hr., (G) 400°C, 2 hr., (H) 500°C, 2 hr (from reference III.59).

E), the broad peaks for γ-Fe_2O_3 appear in addition to those for γ-FeOOH, and in the 200°C-treated sample (sample F), all the peaks change into those for γ-Fe_2O_3. When fine particles of γ-FeOOH had been treated at temperatures higher than 400°C, the products were transformed into the more stable α-Fe_2O_3 (samples G and H) (III.69, III.70). It should be mentioned that in the diffraction peaks in sample F, there is a significant difference in the half-width. The crystallite size estimated from the half-width of sample F is 5, 12, and 11 nm for the (311), (400) and (440) peaks, respectively, and it is suggestive of an anisotropy of the crystallite shape in the decomposed product. Nakajima and coworkers explain such anomalous X-ray line broadening by the formation of the stacking faults in the spinel structure of γ-Fe_2O_3 (III.71).

Efforts were made to obtain crystal size from TEM pictures to compare to the particle shape indicated by XRD; however, the pictures could only be used to provide qualitative agreement between XRD and TEM.

III.H.3. Mechanism of Thermal Decomposition of γ-FeOOH Particles

Giovanoli and Brütsch reported "that the γ-Fe_2O_3 in partly decomposed crystals of γ-FeOOH is not a single crystal but a polycrystalline aggregate so perfectly oriented that its texture pattern could be mistaken for a single crystal electron diffraction" (III.63; III.64). The same thing has been pointed out previously by Takada and coworkers (III.61; III.62). It may be expected from these diffraction studies that there is a high regularity in the process of decomposition of γ-FeOOH. The mechanism of thermal decomposition will be discussed based on the porous texture and the topotactic relation between γ-FeOOH and γ-Fe_2O_3.

Orthorhombic lepidocrocite, γ-FeOOH, has the cell dimensions a_o = 1.24 nm, b_o = 0.387 nm, and c_o = 0.306 nm, while cubic maghemite, γ-Fe_2O_3, has the cell dimension a_o = 0.83 nm (III.72). The change in crystal lattice due to the decomposition of γ-FeOOH into γ-Fe_2O_3 is diagrammatically shown in Figure III.43 on

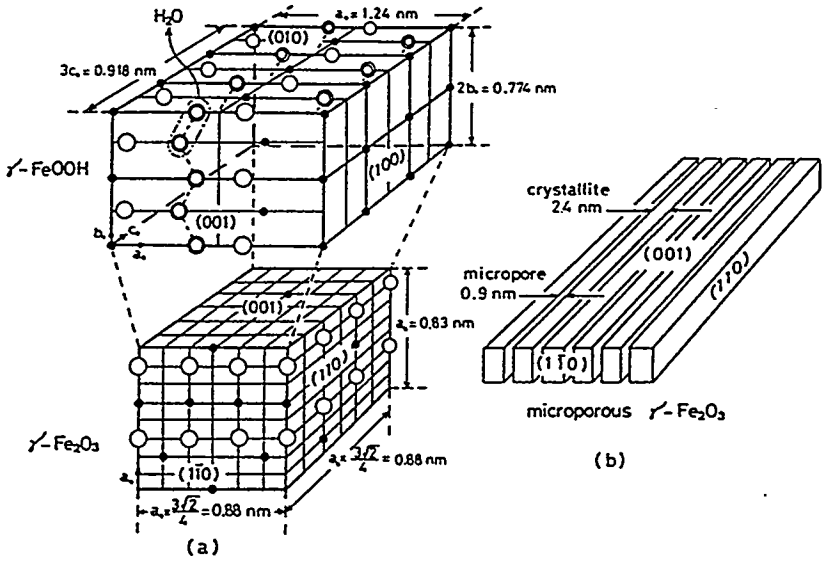

Figure III.43. (a) Topotactic relation between γ-FeOOH and γ-Fe_2O_3 and (b) model of microporous γ-Fe_2O_3 (from reference III.59).

the basis of the topotactic relationship established so far (III.53). From Figure III.43, the change in lattice size of γ-FeOOH is calculated as:

[100]	29.1% contraction
[010]	7.2% elongation
[001]	4.3% contraction

The decomposition of γ-FeOOH takes place by condensation-dehydration of hydroxide ions which are arranged parallel to the (100) plane of γ-FeOOH. Many vacancies are formed on the flat (010) surface of γ-FeOOH by dehydration. γ-FeOOH

crystal lattice contracts along the [100] direction so as to fill the vacancies. As a result of such contraction, the slit-shaped micropores and the plate-like crystallites of γ-Fe_2O_3 are expected to be formed in the matrix particle. The width of micropores has been determined by the analysis of the nitrogen isotherm to be 0.9 nm. To form the slit-shaped micropore of 0.9 nm in width, it is calculated from Figure III.43 that the plate-like γ-Fe_2O_3 crystallites of 2.4 nm in thickness are formed in the matrix particles. The model of microporous γ-Fe_2O_3 obtained in this way is depicted in Figure III.43.

Other significant information about the decomposition may be obtained by measuring the Kr adsorption on the surface of partially decomposed particles of γ-FeOOH. As is shown in Figure III.32, the step due to the homogeneity of the (010) surface of γ-FeOOH decreases rapidly with the progress of decomposition. This fact strongly suggests that the decomposition reaction proceeds preferentially on the (010) surface of γ-FeOOH. The formation of micropores due to dehydration transforms the homogeneous surface into a heterogeneous one. In conclusion, in the thermal decomposition reaction of γ-FeOOH, the nuclei of γ-Fe_2O_3 (2.4 nm in thickness) are initially formed on the (010) surface of γ-FeOOH, and the nuclei of the same size are successively formed along the [010] direction of γ-FeOOH until the decomposition is completed. Giovanoli and Brütsch (III.63; III.64) estimated the size of γ-Fe_2O_3 nuclei to be 7 nm. Their large value might be due to the similar effect of the electron beam as mentioned before in the determination of pore size.

The surface area following heat treatments of 2 hours indicate that the area attains a maximum upon heating to about 200°C and then declines with heating at higher temperatures (Figure III.44).

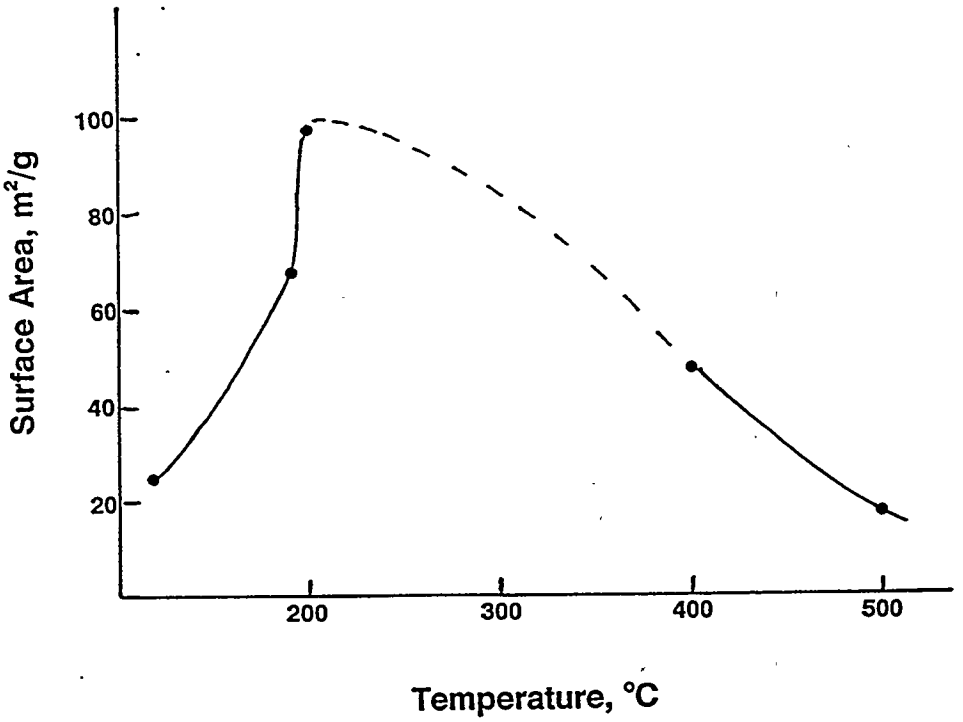

Figure III.44. Surface area of γ-FeOOH decomposition products after heating at increasing temperatures (data from reference III.59).

III.H.4. Transformation of δ-FeOOH

Francombe and Rooksby (III.66) followed the transformation of δ-FeOOH. They found that it transforms to geothite on heating at about 150°C, but the transformation is incomplete due to a tendency to lose water directly to the atmosphere. The water loss with temperature increase is illustrated in Figure III.45. From the X-ray powder data these authors concluded that the ferric ions occupy the interstices of the anion lattice in such a way that approximately 80% of the iron is

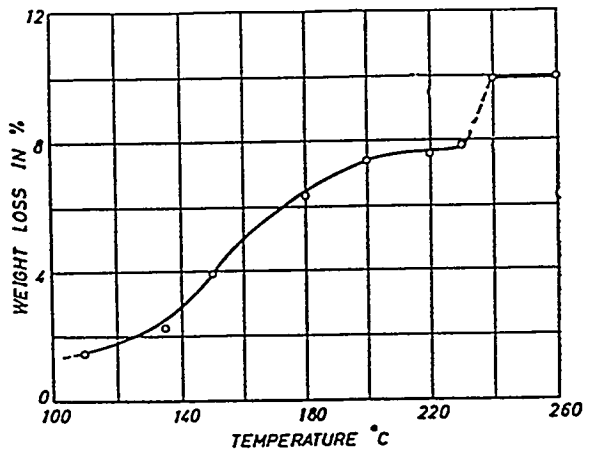

Figure III.45. Weight loss on heating δ-FeOOH at different temperatures for two hour periods (from reference III.66).

randomly distributed in octahedral sites, while the remainder is placed primarily in tetrahedral sites. The authors state that this cation distribution enables both the transformation to geothite and the magnetic properties to be satisfactorily explained.

With a poorly crystallized δ-FeOOH, two hours at 150°C in air was sufficient to substantially complete the dehydration. For a better crystallized δ-FeOOH, dehydration is only 40% complete, and part of the material was converted to geothite (Figure III.45). When the temperature was raised to about 220°C no noticeable increase in the proportion of geothite was observed but the dimensions of the δ structure change progressively with temperature with heating, as shown in Figure III.46 (in this paper the authors use the older nomenclature of δ-Fe_2O_3 and α-Fe_2O_3 at times rather than δ-FeOOH and α-FeOOH). After heating at 240°C the δ-structure is substantially transformed to a disordered form of hematite.

The behavior is modified if the δ-FeOOH is heated in water in a sealed tube (autogeneous water pressure). The sequence of changes is still the same but conversion to geothite is nearly complete at 150°C.

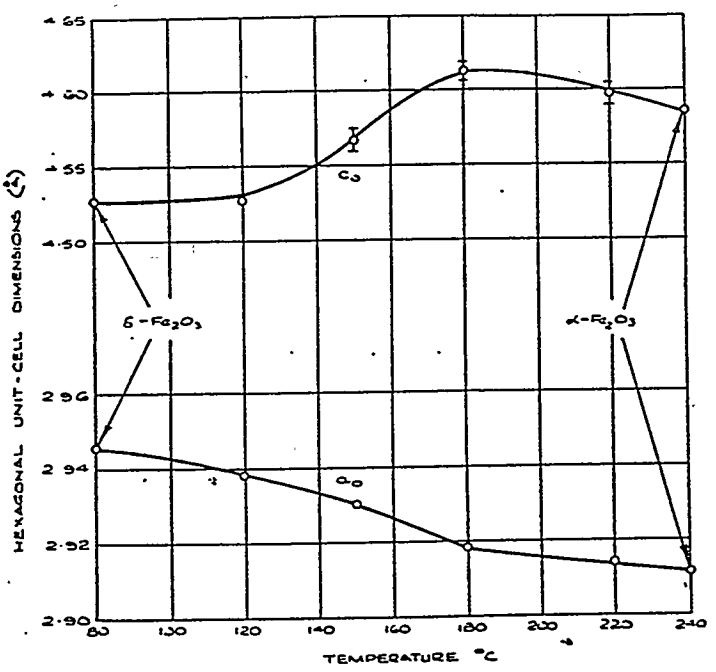

Figure III.46. Variation of unit-cell dimensions on heating δ-FeOOH at different temperatures for two hour period (from reference III.66).

III.I Summary of Preparation/Transformation

The preparation of a single phase of FeOOH may be very complex so that a variety of final products may result depending upon the conditions employed in the preparation procedures. For example, the pH and temperature of precipitation/aging lead to a range of crystal sizes of α-FeOOH, α-Fe_2O_3 or mixtures of these; some possible pathways determined by these variables are outlined in the following diagram (Figure III.47).

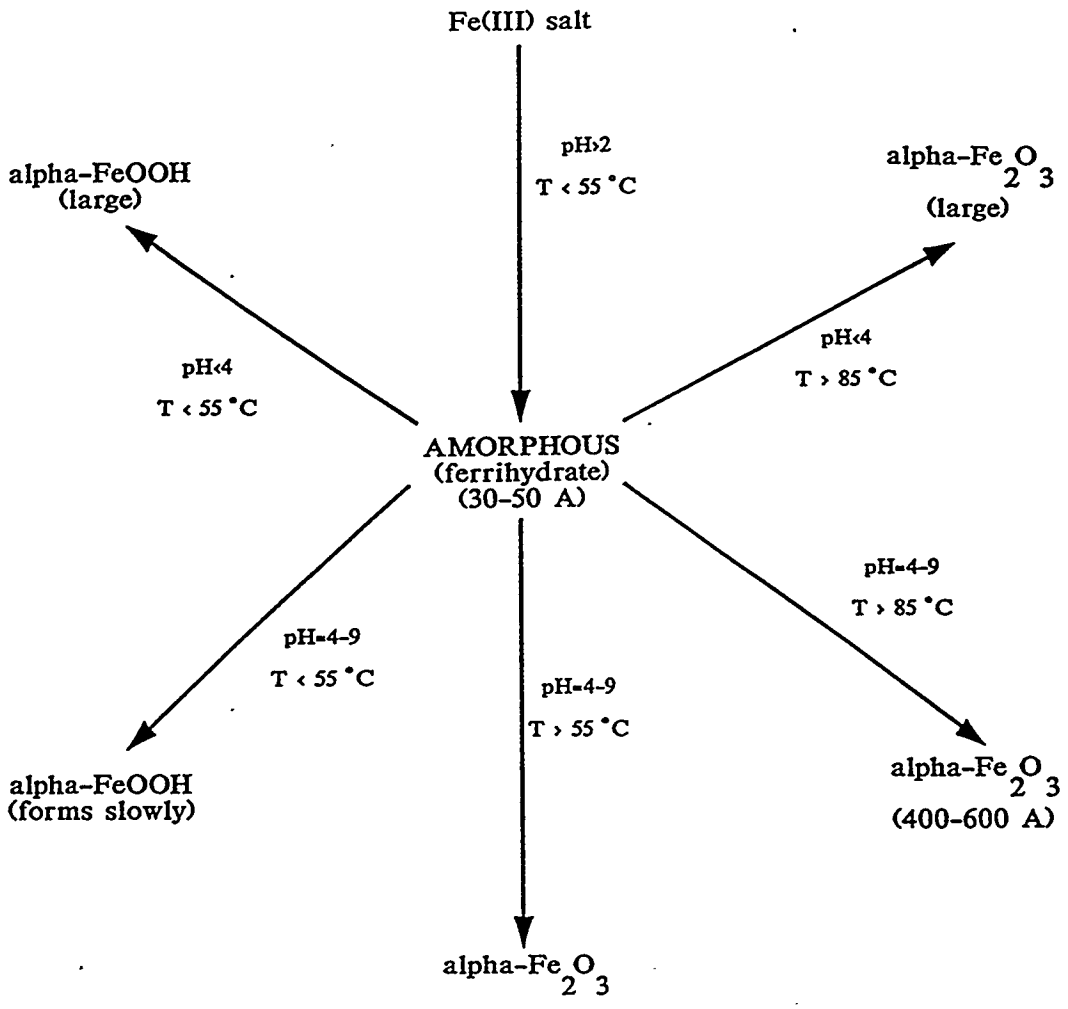

Figure III.47. Dependence upon product structure and crystal size upon preparation parameters.

The structural transformations of the iron oxide/hydroxide system with changes in oxidation, dehydration and heating have been summarized by Bernal et al. (III.68). Schematically, these are summarized in Figure III.48. It is noted that the α structure, for both FeOOH and Fe_2O_3, is the most stable. The common characteristics of the oxyhydroxides and the oxides are summarized in Table III.8.

Table III.8

Characteristics of "Hydrous" Iron Oxides or Oxyhydroxides

Formula	Mineral (Common Name)	Crystal System	Crystal Structure	Unit Cell Dimensions (nm)	Color	Decompose
$Fe_5HO_8 \cdot 4H_2O$	Ferrihydrite	Hexagonal	Defect Corundum	a=0.508, c=0.94		
α-FeOOH	Geothite	Orthorhombic	Diaspore (rhombhredron)	a=0.4608, b=0.9956,	Brown to blackish	-1/2 H_2O, 126
β-FeOOH	Akaganéite	Tetragonal	Hollandite[a]	a=1.053, c=0.303		
γ-FeOOH	Lepidocrocite	Orthorhombic	Boehmite (orthorhombic)	a=0.388, b=1.254,		~140-180
δ-FeOOH		Hexagonal	CdI_2 (hexagonal)	a=0.293, c=0.460		~80-240
δ'-FeOOH	Feroxyhite	Hexagonal	Disordered CdI_2	a=0.293, c=0.460		
ϵ-FeOOH		Orthorhombic	InOOH	a=0.4937, b-0.4432, c=0.2994		
FeO	Wüstite	Cubic	Defect NaCl (cubic)	a=0.428 - 0.431	Black	
Fe_3O_4	Magnetite	Cubic	Inverse Spinel (cubic)	a=0.8391	Black	
α-Fe_2O_3	Hematite	Hexagonal	Corundum (trigonal)	a=0.5034, c=1.3752	Reddish brown to black	
γ-Fe_2O_3	Maghemite	Cubic or tetragonal	Defect Spinel	a=0.834		

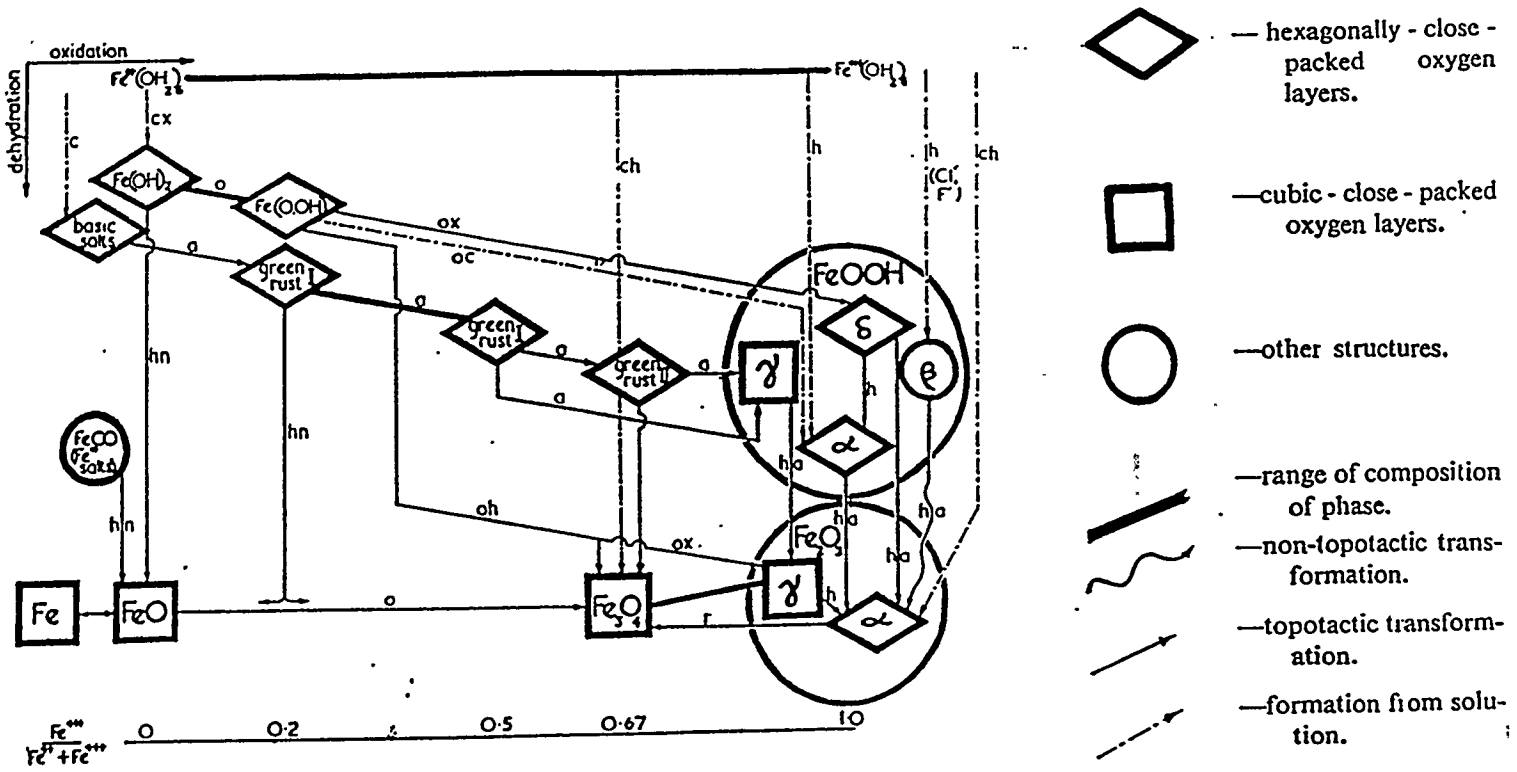

Figure III.48. Structural transformations in the iron oxide/hydroxide system. a - on exposure to air; c - in alkali; h - on heating; n - in nitrogen or *in vacuo*; o - on oxidation; r - on reduction; x - in excess (from reference III.68).

III.J. Iron Oxides

Three oxides of iron may be distinguished, but are all subject to nonstoichiometry (III.104, III.105). The lowest is FeO which may be obtained by heating iron in a low partial pressure of O_2 or as a fine, black pyrophoric powder by heating iron(II) oxalate *in vacuo*. Below about 575°C it is unstable towards disproportionation into Fe and Fe_3O_4 but can be obtained as a metastable phase if cooled rapidly. It has a rock salt structure but is always deficient in iron, with a homogeneity range of $Fe_{0.84}O$ to $Fe_{0.95}O$.

Fe_3O_4 is a mixed Fe^{II}/Fe^{III} oxide which can be obtained by partial oxidation of FeO or, more conveniently, by heating Fe_2O_3 above about 1400°C. It has the inverse

spinel structure. Spinels are of the form $M^{II}M_2^{III}O_4$, and in the normal spinel the oxide ions form a ccp lattice with M^{II} ions occupying tetrahedral sites and M^{III} ions octahedral sites. In the inverse structure half the M^{III} ions occupy tetrahedral sites, with the M^{II} and the other half of the M^{III} occupying octahedral sites. Fe_3O_4 occurs naturally as the mineral magnetite or lodestone. It is a black, strongly ferromagnetic substance (or, more strictly, "ferrimagnetic"), insoluble in water and acids. Its electrical properties are not simple, but its rather high conductivity may be ascribed to electron transfer between Fe^{II} and Fe^{III}.

Fe_2O_3 is known in a variety of modifications of which the more important are the α- and γ-forms. When aqueous solutions of iron(III) are treated with alkali, a gelatinous reddish-brown precipitate of hydrated oxide is produced. When heated to 200°C, this gives the red-brown α-Fe_2O_3. This has the corundum structure in which the oxide ions are hcp and the metal ions occupy octahedral sites. It occurs naturally as the mineral haematite.

The interconvertibility of FeO, Fe_3O_4, and γ-Fe_2O_3 arises because of their structural similarity. Unlike α-Fe_2O_3, which is based on a hcp lattice of oxygen atoms, these three compounds are all based on ccp lattices of oxygen atoms. In FeO, Fe^{II} ions occupy the octahedral sites and nonstoichiometry arises by oxidation, when some Fe^{II} ions are replaced by two-thirds their number of Fe^{III} ions. Continued oxidation produces Fe_3O_4 in which the Fe^{II} ions are in octahedral sites, but the Fe^{III} ions are distributed between both octahedral and tetrahedral sites. Eventually, oxidation leads to γ-Fe_2O_3 in which all the cations are Fe^{III} which are randomly

distributed between octahedral and tetrahedral sites. The oxygen lattice remains intact throughout but contracts somewhat as the number of iron atoms which it accommodates diminishes.

REFERENCES - Section III

III.1. J. Cornejo, C. J. Serna and M. C. Hermosin, *J. Coll. Interface Sci.*, **102**, 101 (1984).

III.2. A. A. Van der Giessen, *J. Inorg. Nucl. Chem.*, **28**, 2155 (1966).

III.3. K.-H. Towe and W. P. Bradley, *J. Coll. Interface Sci.*, **24**, 384 (1967).

III.4. F. V. Chukhrov, B. B. Zuyagin, L. P. Ermilova and A. I. Gorshokv, in "Proc. Int. Clay Conf., Madrid, 1972", (J. M. Serratosa, Ed.), pg. 333.

III.5. J. D. Russell, *Clay Miner.*, **14**, 109 (1979).

III.6. U. Schwertmann and W. R. Fisher, *Geoderma*, **10**, 237 (1973).

III.7. S. Brunauer, L. S. Deming, W. E. Deming and E. Teller, *J. Am. Chem. Soc.*, **62**, 1723 (1940).

III.8. J. H. de Boer in "The Structure and Properties of Porous Materials," (H. Everett and F. S. Stone, Eds.), Butterworths, London, 1958.

III.9. D. Dollimore and G. R. Heal, *J. Colloid Interface Sci.*, **33**, 508 (1964).

III.10. W. R. Fisher and U. Schwertmann, *Clays & Clay Miner.*, **23**, 33 (1975).

III.11. J. H. A. Van der Woude and P. L. de Bruyn, *Colloids and Surfaces*, **8**, 55 (1983).

III.12. J. H. A. Van der Woude, P. Verhees and P. L. de Bruyn, *Colloids and Surfaces*, **8**, 79 (1983).

III.13. J. Dousma and P. L. de Bruyn, *J. Coll. Interface Sci.*, **56**, 527 (1976).

III.14. T. P. L. M. Feenstra and P. L. de Bruyn, *J. Phys. Chem.*, **83**, 475 (1979).

III.15. A. E. Nielsen, "Kinetics of Precipitation", Pergamon Press, New York, NY, 1964.

III.16. A. C. Makrides, M. Turner and J. Slaughter, *J. Colloid Interface Sci.*, **73**, 845 (1980).

III.17. Th. G. Spiro, S. E. Allerton, J. Renner, A. Terzis, R. Bils and P. Saltman, *J. Am. Chem. Soc.*, **38**, 2721 (1966).

III.18. R. A. Buyanov, O. P. Krivornuchko and I. A. Ryzhak, *Kinet. Katal.*, **13**, 470 (1972).

III.19. J. Dousma and P. L. de Bruyn, *J. Colloid Interface Sci.*, **64**, 154 (1978).

III.20. B. A. Sommer, D. W. Margerum, J. Renner, P. Saltman and T. G. Spiro, *Bioinorg. Chem.*, **2**, 295 (1973).

III.21. R. C. Mackenzie and R. Meldau, *Mineral. Mag.*, **32**, 153 (1959).

III.22. U. Schwertmann, W. R. Fisher, H. Papendorf, *Trans. 9th Intern. Congr. Soil Sci.*, 645 (1968).

III.23. K. Wefers, *Ber. Dtsch. Keram. Ges.*, **43**, 677 (1966).

III.24. A. Norlund Christensen, P. Convert and M. S. Lehmann, *Acta Chem. Scand.*, **A34**, 771 (1980).

III.25. J. Dousma and P. L. de Bruyn, *J. Colloid Interface Sci.*, **72**, 314 (1979).

III.26. S. Okamoto, H. Sekizawa and S. I. Okamoto, in "Reactivity of Solids; Proc. 7th Int. Symp. on the Reactivity of Solids" (J. S. Anderson, M. W. Roberts and F. S. Stone, Eds.), Chapman and Hall, London, 1972, pp 341-353.

III.27. J. H. L. Waton, W. Heller, and W. Wojtowicz, *J. Chem. Phys.*, **16**, 997 (1948).

III.28. J. H. L. Watson, R. R. Cardell,Jr., and W. Heller, *J. Phys. Chem.*, **66**, 1757 (1962).

III.29. A. L. Mackay, *Mineral Mag.*, **33**, 270 (1962).

III.30. J. F. Kerridge, in "Proceedings of the 3rd European Regional Conference on Electron Microscopy", p. 355, 1964.

III.31. R. Söderquist and S. Jansson, *Acta Chem. Scand.*, **20**, 1417 (1966).

III.32. R. H. H. Wolf, M. Wrisher, and J. Šipalo-Zuljević, *Kolloid-Z.Z. Polym.*, **215**, 57 (1967).

III.33. N. Yamamoto, T. Shinjo, M. Kiyama, Y. Bando, and T. Takada, *Phys. Soc. Japan*, **25**, 1267 (1968).

III.34. J. T. Kenney, W. P. Townsend, and J. A. Emerson, *Colloid Interface Sci.*, **42**, 589 (1973).

III.35. J. Ellis, R. Giovanoli, and W. Stumm, *Chimia*, **30**, 194 (1976).

III.36. K. J. Gallagher, *Nature*, **226**, 1225 (1970).

III.37. Y. Maeda and S. Hachisu, *Colloids and Surfaces*, **7**, 357 (1983).

III.38. T. G. Spiro, L. Pape, and P. Saltman, *J. Amer. Chem. Soc.*, **89**, 5555 (1967); T. G. Spiro, S. E. Allerton, J. Renner, A. Terzis, R. Bills, and P. Saltman, *J. Amer. Chem. Soc.*, **88**, 2721 (1966).

III.39. E. Matijević, R. S. Sapieszko and J. B. Melville, *J. Colloid Interface Sci.*, **50**, 567 (1975).

III.40. R. S. Sapieszko, R. Patel and E. Matijević, *J. Phys. Chem.*, **81**, 1061 (1977).

III.41. E. Matijević and P. Scheiner, *J. Colloid Interface Sci.*, **63**, 509 (1978).

III.42. J. Babćan, *Geol. Carpathica*, **22**, 11 (1971).

III.43. W. Feitknecht and W. Michaelis, *Helv. Chim. Acta*, **45**, 212 (1962).

III.44. U. Schwertmann, *Z. Anorg. Allgem. Chem.*, **298**, 337 (1959).

III.45. B. Weiser and W. O. Milligan, *J. Phys. Chem.*, **39**, 25 (1935).

III.46. D. R. Dasgupta and A. L. Mackay, *J. Phys. Soc. Japan*, **14**, 932 (1959).

III.47. J. D. Bernal, D. R. Dasgupta and A. L. Mackay, *Clay Miner. Bull.*, **4**, 15 (1959).

III.48. G. Butler and H. C. K. Ison, *Chem. Commun.*, **12**, 264 (1965).

III.49. K. M. Parida, *J. Mat. Sci. Lett.*, **6**, 1476 (1987).

III.50. B. H. Davis, unpublished results.

III.51. J. D. Bernal, D. R. Dasgupta and A. L. Mackay, *Clay Miner. Bull.*, **4**, 15 (1959).

III.52. T. Misawa, K. Hashimoto and S. Shimodaira, *J. Inorg. Nucl. Chem.*, **35**, 4159 (1973).

III.53. T. Misawa, K. Hashimoto and S. Shimodaira, *J. Inorg. Nucl. Chem.*, **35**, 4167 (1973).

III.54. Y. Tamaura, M. Saturno, K. Yamada and T. Katsura, *Bull. Chem. Soc. Japan*, **57**, 2417 (1984).

III.55. T. F. Barton, T. Price and J. G. Dillard, *J. Coll. & Interface Sci.*, **141**, 553 (1991).

III.56. T. F. Barton, T. Price and J. G. Dillard, *J. Coll. & Interface Sci.*, **138**, 122 (1990).

III.57. T. Misawa, K. Hashimoto and S. Shimodaira, *Corros. Sci.*, **14**, 131 (1974).

III.58. A. Mackay in "Reactivity of solids", (J. deBoer et al., Eds.) Elsevier, Amsterdam, 1961, pg. 571.

III.59. H. Naono and K. Nakai, *J. Colloid. & Interface Sci.*, **128**, 146 (1989).

III.60. M. Kiyama, T. Akita and T. Takada, *Bull. Inst. Chem. Res. Kyoto Univ.*, **61**, 335 (1983).

III.61. T. Takada, M. Kiyama and S. Shimizu, *Bull. Inst. Chem. Res. Kyoto Univ.*, **42**, 505 (1964).

III.62. T. Takada, K. Nagasawa, M. Kiyama, S. Shimizu and Y. Bando, *Bull. Inst. Chem. Res. Kyoto Univ.*, **47**, 600 (1969).

III.63. R. Giovanoli and R. Brütsch, *Chimia*, **28**, 188 (1974).

III.64. R. Giovanoli and R. Brütsch, *Thermochim. Acta*, **13**, 15 (1975).

III.65. E. S. Dana, "A Textbook of Mineralogy" (Modern Asia, Ed.) Wiley, Tokyo, p. 504 (1960).

III.66. M. H. Francombe and H. P. Rooksby, *Clay Minerals Bull.*, **4 (21)**, 1, (1959).

III.67. O. Glemser and E. Gwinner, *Z. Anorg. Chem.*, **240**, 163 (1939).

III.68. J. D. Bernal, D. R. Dasgupta and A. L. Mackay, *Clay Minerals Bull.*, **4**, 15 (1959).

III.69. A. A. Olowe, Ph. Refait and J. M. R. Génin, *Corrosion Sci.*, **32**, 1003 (1991).

III.70. T. Misawa, T. Kyuno, W. Suétaka and S. Shimodaira, *Corrosion Sci.*, **11**, 35 (1974).

III.71. S. Okamoto, *J. Amer. Ceram. Soc.*, **51**, 594 (1968).

III.72. O. Muller, R. Wilson and W. Krakow, *J. Material Sci.*, **14**, 2929 (1979).

III.73. A. A. Olowe, Thesis, Nancy, France (1988).

III.74. J. M. R. Génin, D. Rézel, Ph. Bauer, A. Olowe and A. Beral, *Electrochem. Methods in Corros. Research, Materials Sci. Forum*, **8**, 477 (1986).

III.75. D. R. Rézel, Thesis, Nancy I, France (1988).

III.76. E. Murad and U. Schwertmann, *Clay Minerals*, **18**, 301 (1980).

III.77. A. Krause and A. Borkowska, *Roczn. Chemii*, **29**, 999 (1955).

III.78. A. A. Olowe and J. M. R. Génin, *Corrosion Science*, **32**, 965 (1991).

III.79. O. Baudisch and P. Mayer, *Biochem. Z.*, **107**, 1 (1920).

III.80. S. Okamoto, *J. Am. Ceram. Soc.*, **51**, 54 (1968), ASTM card no. 22-346.

III.81. F. A. Cotton and G. Wilkinson, *Advanced Inorganic Chemistry*, 2nd ed., p. 858, John Wiley & Sons, 858 (1966).

III.82. P. Schindler, W. Michaelis and W. Feitknecht, *Helv. Chim. Acta*, **46**, 444 (1963).

III.83. A. M. Van der Kraan and J. Medema, *J. Inorg. Nucl. Chem.*, **31**, 2039 (1969).

III.84. V. Frei, *Coll. Czech. Chem. Commun.*, **27**, 775 (1962).

III.85. E. Murad and U. Schwertmann, *Am. Mineral.*, **65**, 1044 (1980).

III.86. K. M. Towe and W. F. Bradley, *J. Colloid Interface Sci.*, **24**, 384 (1967).

III.87. A. A. Olowe, Ph. Bauer and J. M. R. Génin, *Hyperfine Interactions*, **41**, 501 (1988).

III.88. A. A. Olowe, D. Rézel and J. M. R. Génin, *Hyperfine Interactions*, **46**, 429 (1989).

III.89. Y. Tamaura, C. Kameshima and T. Katsura, *J. Electrochem. Soc.*, **128**, 1447 (1981).

III.90. M. Kiyama, *Bull. Chem. Soc. Jpn.*, **47**, 1646 (1974).

III.91. J. E. O. Mayne, *J. Chem. Soc.*, 129 (1953).

III.92. J. E. Hiller, *Werkst. Korros.*, **11**, 943 (1966).

III.93. H. Schwartz, *Werkst. Korros.*, **23**, 648 (1972).

III.94. A. Girard and G. Chaudron, *Comptes Rendus Acad. Sci. Paris*, **200**, 127 (1935).

III.95. G. W. ban Oosterhout, *J. Inorg. Chem.*, **29**, 1235 (1967).

III.96. M. François and J. P. Martiny, Institut de Chim. Ind., U.L.B., Rapport Interne (1972).

III.97. R. Derie and M. Ghodsi, *Ind. Chim. Belg.*, **37**, 731 (1972).

III.98. J. Detournay, M. Ghodsi and R. Derie, *Ind. Chim. Belg.*, **39**, 695 (1974).

III.99. A. A. Olowe, J. M. R. Génin and Ph. Bauer, *Hyperfine Interactions*, **46**, 437 (1989).

III.100. W. Feitknecht and G. Keller, *Z. Anorg. Chem.*, **262**, 61 (1950).

III.101. J. Detournay, L. de Miranda, R. Derie and M. Ghodsi, *Corros. Sci.*, **15**, 295 (1975).

III.102. J. R. Gancedo, M. L. Martinez and J. M. Olton, *J. de Phys., Colloque C6, Suppl. Au No. 12*, **37**, 297 (1976).

III.103. Y. Tamaura, T. Yoshida and T. Katsura, *Bull. Chem. Soc. Jpn.*, **57**, 2144 (1984).

III.104. N. N. Greenwood, in "Ionic Crystals, Lattice Defects and Nonstoichiometry", Chap. 6, Butterworths, London, 1968, pp 111-47.

III.105. N. N. Greenwood and A. Earnshaw, "Chemistry of the Elements", Permagon Press, Oxford, 1984.